

Real-time measurement of temperature for control of laser surface modification process

S. Ahn, J. Murphy, J. A. Ramos, K. Wood, J. J. Beaman
Laboratory for Freeform Fabrication
Department of Mechanical Engineering
The University of Texas at Austin, Austin, TX 78712

Abstract

The process of laser surface modification is a complex transient three-dimensional heat conduction problem. A moving heat source and a moving phase boundary further complicate the modeling. This general problem can be simplified using appropriate assumptions resulting in an energy balance equation used to derive a melt depth model as a function of interaction time and laser power input. The model can then be used to design and implement a real-time feedback control scheme. The measurement used for feedback to the control algorithm is the surface temperature. The real-time surface temperature measurements are obtained by using a unique pyrometer arrangement. This measurement scheme allows the pyrometer measurement aperture to directly follow the laser beam path through the entire surface modification process in real-time. Experiments using a Nd:YAG laser were performed on mild steel samples to verify the suggested model's results.

Introduction

For a successful laser surface modification process such as surface hardening and remelting, the heat affected zone depth or the melt depth is an important quantity [1-4]. The processing results depend on those parameters and should be controlled in real-time during the process. But these quantities are immeasurable during the process. Instead we can measure the maximum surface temperature by using infrared pyrometer. An appropriate model is required to relate the surface temperature measurement to the melt depth. Previously, a one-dimensional melting model [2] was developed, but the difficulty in deriving the relationship between the melt depth and the surface temperature impaired its usefulness for real-time control applications. The proposed model calculates the melt depth based on the energy balance equation proposed by Pantelis and Vonatsos [3]. Once the melt depth is known, the surface temperature can be obtained from Xie and Kar's model [4]. To verify the model, single-line scan experiments were performed on mild steel plates (SAE 1010 cold drawn). The samples were then cross-sectioned and melt depth measurements were taken. The results were compared with the data from the model simulations. Surface temperature measurements taken during the experiments were also compared with the simulation results.

Physical modeling

The proposed model for calculating the melt depth as a function of power input and the interaction time does not consider the thermal field in the material, which is a significant change from the previous modeling effort [2]. For the model to be obtained, the following assumptions are made [3]:

1. The incident laser beam heats up the surface so quickly that melting occurs instantly.
2. The material melts simultaneously over the entire spot surface and the horizontal liquid-solid interface remains flat.
3. Laser melted zone has constant temperature everywhere equal to T_m .
4. The depth L , where the material again reaches temperature equal to T_{inf} , is proportional to the depth of the molten pool.
5. The heat affected zone is modeled as a moving front with temperature $T_1=(T_m-T_{inf})/2$.
6. The maximum temperature does not exceed the melting temperature.

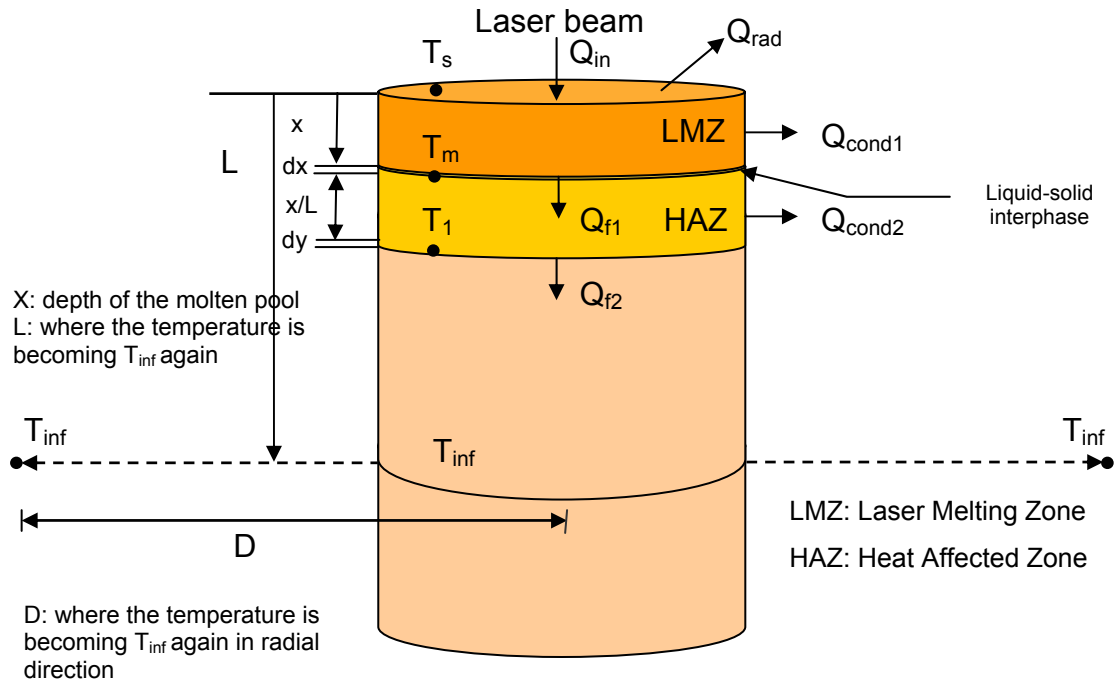


Fig. 1: The schematic illustration of the model

On the assumption that the depth of the molten pool is equal to x , the moving front (heat affected zone) is at distance x/L from the end of the molten pool. So, if $u = dx/dt$ describes the velocity of the front of the molten pool, the moving front has a velocity equal to $\frac{(L+1) dx}{L dt}$. The movement of the front of the molten pool is equivalent to a heat flux;

$$Q_{f1} = (\rho C_p(T_m)T_m A_m + \rho A_m L_m) \frac{dx}{dt} \quad (1)$$

Similarly, the moving front is equivalent to a heat flux;

$$Q_{f2} = \rho C_p(T_1)T_1 A_m \frac{L+1}{L} \frac{dx}{dt} \quad (2)$$

The rates of heat losses due to conduction at the LMZ and at the HAZ are respectively,

$$Q_{cond1} = 2\pi k(T_m - T_\infty) \frac{x}{\ln(D/d_m)} \quad (3)$$

$$Q_{cond2} = 2\pi k(T_1 - T_\infty) \frac{x}{L \ln(D/d_m)} \quad (4)$$

Where, D is the radial distance at which the material is at room temperature, T_{inf} . Ghosh and Malik suggest that $D/d \approx 55$ [5]. By using this numerical values the equations become

$$Q_{cond1} = \pi k(T_m - T_\infty) \frac{x}{2} \quad (5)$$

$$Q_{cond2} = \pi k(T_1 - T_\infty) \frac{x}{2L} \quad (6)$$

Also, there is radiant heat transfer at the surface equal to

$$Q_{rad} = \sigma A_m T_m^4 \quad (7)$$

The input uniform heat flux $Q_{in} = AP$ where A is absorptivity of the material and P is laser power input (W). Therefore due to energy balance, the following equation is obtained.

$$Q_{in} = Q_{f1} + Q_{f2} + Q_{cond1} + Q_{cond2} + Q_{rad} \quad (8)$$

and it leading to

$$\dot{x} = -\frac{q_1}{q_2} x + \frac{q_3}{q_2} \quad (9)$$

where,

$$q_1 = \pi k \frac{T_1 - T_\infty}{2LA_m} + \pi k \frac{T_m - T_\infty}{2A_m} \quad (9a)$$

$$q_2 = \rho C_p(T_m)T_m + \rho C_p(T_1)T_1 \frac{L+1}{L} + L_m \rho \quad (9b)$$

$$q_3 = \frac{AP}{A_m} - \sigma T_m^4 \quad (9c)$$

with initial condition for $x=0$ ($t=0$). We now have melt depth as a function of the power input.

Once the melt depth is estimated, x_0 , it is possible to calculate the surface temperature based on Xie and Kar's model [4]. From Xie and Kar, the 2nd order temperature profile for liquid region is:

$$T_l(x, t) = T_m - \frac{AI}{k_l} [x - x_0(t)] + \frac{AI}{2\alpha_l k_l \left[1 + \frac{x_0(t)}{\alpha_l} \dot{x}_0(t) \right]} \dot{x}_0(t) [x^2 - x_0^2(t)], 0 \leq z \leq x_0(t) \quad (10)$$

Substituting $x=0$ results in the following equation for the surface temperature.

$$T_s(t) = T_m + \frac{AI}{k_l} x_0(t) - \frac{AI \dot{x}_0(t) x_0^2(t)}{2\alpha_l k_l \left[1 + \frac{x_0(t)}{\alpha_l} \dot{x}_0(t) \right]} \quad (11)$$

By using Eq. 9 and Eq. 11 in combination, melt depth can be estimated by surface temperature measurement, and the depth can be controlled using the laser power input.

Simulation and Experiments

For the experimental validation of the thermal model mild steel plates (WxDxH: 25x50x7 [mm]) were scanned using a Nd:YAG laser (U.S. Lasers, max. power 600W, 1064nm). To measure the surface temperature in real-time, a pyrometer (Raytek, Marathon MA2SC, 1 ms response time, Temperature range 623K-2273K, 1600nm) was installed. The temperature signal was isolated using a short wave pass filter (VLOC, 99.8% R @ 1600nm, 97% T @ 1064nm, at 45 deg. Fused Silica Sub.). A diagram of the experimental setup is shown in Figure 2.

Prior to scanning, the surface of the specimen was prepared using 200-grit sandpaper to create uniform surface roughness and uniform absorptivity. The specimen was processed under rough vacuum ($\sim 10^{-2}$ torr) and backfilled with argon gas to prevent oxidation. The 600 mm focal length lens resulted in a focused beam diameter of 2 mm incident on the specimen.

The two sets of experiments were conducted. The first set of three scans varied the laser power between scans while maintaining a constant scan speed. The power levels used were 350W, 450W, and 550W at a traverse scan speed of 0.27 mm/s. The second set varied the scan speed between scans at a constant power of 550W. The three speeds used were 0.82 mm/s, 0.41 mm/s, and 0.27 mm/s. For both sets of experiments, the specimens were sections at three different locations along the scan path. The three data points for each scan will provide error estimates for the melt depth measurements and will illustrate the effects of heat build up as the scan progresses.

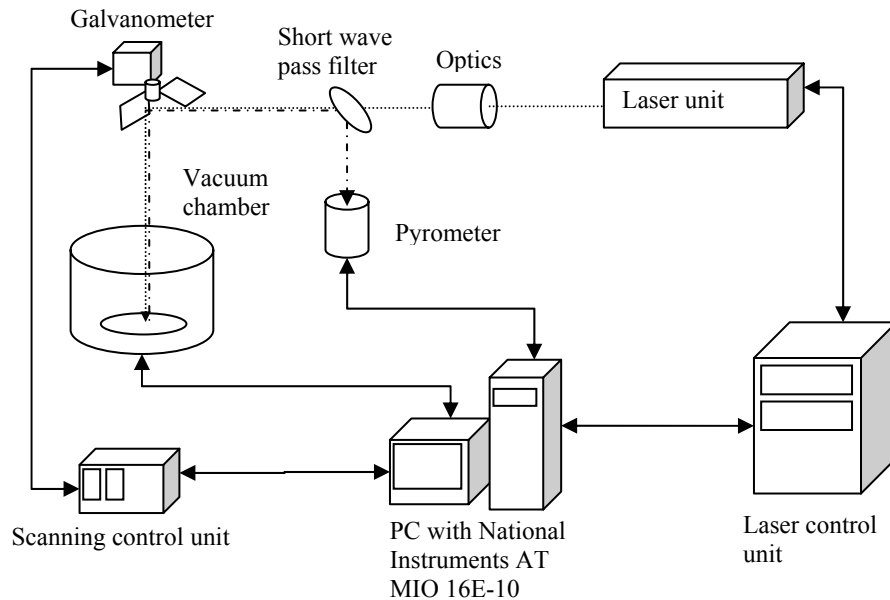


Fig.2: Experimental setup for the laser surface modification process

During the beam scan process, the real-time surface temperature was captured by the pyrometer and recorded to the personal computer with National Instruments DAQ system. After processing, the samples were cut, ground, polished, and etched. For both sets of experiments, the specimens were sectioned at three different locations along the scan path. The three data points for each scan provided error estimates for the melt depth measurements and illustrated the effects of heat build up as the scan progresses.

Melt depth measurements were obtained using an optical microscope with attached CCD camera. The melt depth was estimated by examining the transition in grain structure in the metal.

Results and Discussion

Real-time surface temperature measurement during the scan process was successfully implemented. The short wave pass filter worked as planned, allowing the Nd:YAG laser to be transmitted through and the temperature information to be captured. Figure 4 shows an example of the surface temperature measurement during a scan. In a very short time, the temperature reaches the melting temperature and gradually increases as heat begins to build up.

Figure 5 shown below depicts the relationship between melt depth and interaction time. The interaction time is simply the beam diameter divided by the scan speed. The three scan speeds used in the experiments resulted in the three interaction times shown. The three points at each interaction time represent the three positions where the cross-sections were taken and the melt depth measured. The symbols shown represent the following: “x”- beginning of scan; “o” - middle of scan; “*”- end of scan. As we expected, the melt depth increases when the interaction time is increased. The melt depth also increases within a single scan as the heat builds up. The solid line represents the results of the simulation using the model. The model fits the data well for the

measurements taken at the middle cross section. At the beginning of the scan, the model overestimates the melt depth, and at the end of the scan, the model underestimates the depth.

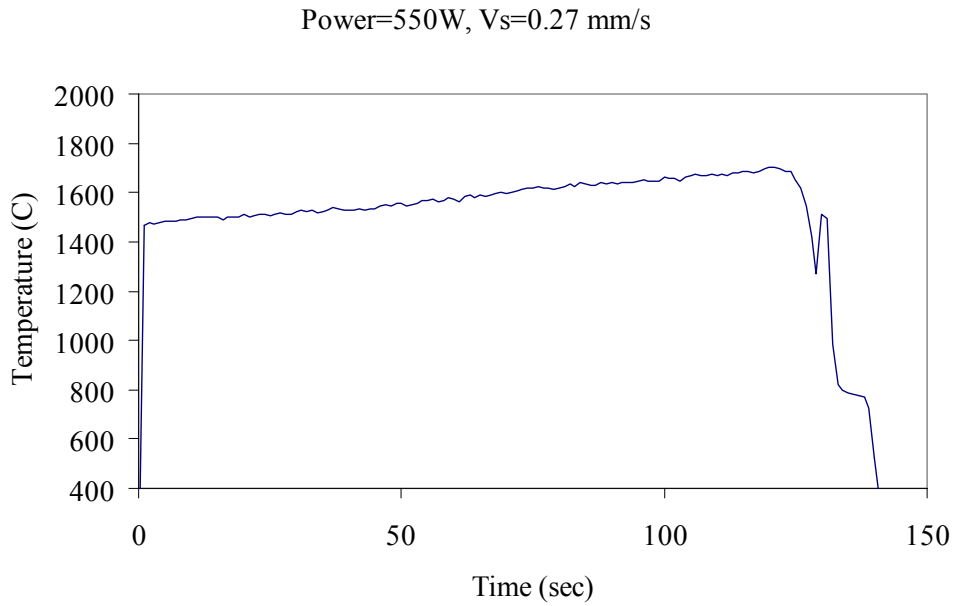


Fig.4: Surface temperature measurement from experiment: Power = 550 W, Vs = .27 mm/s, $T_m=1537\text{ }^\circ\text{C}$

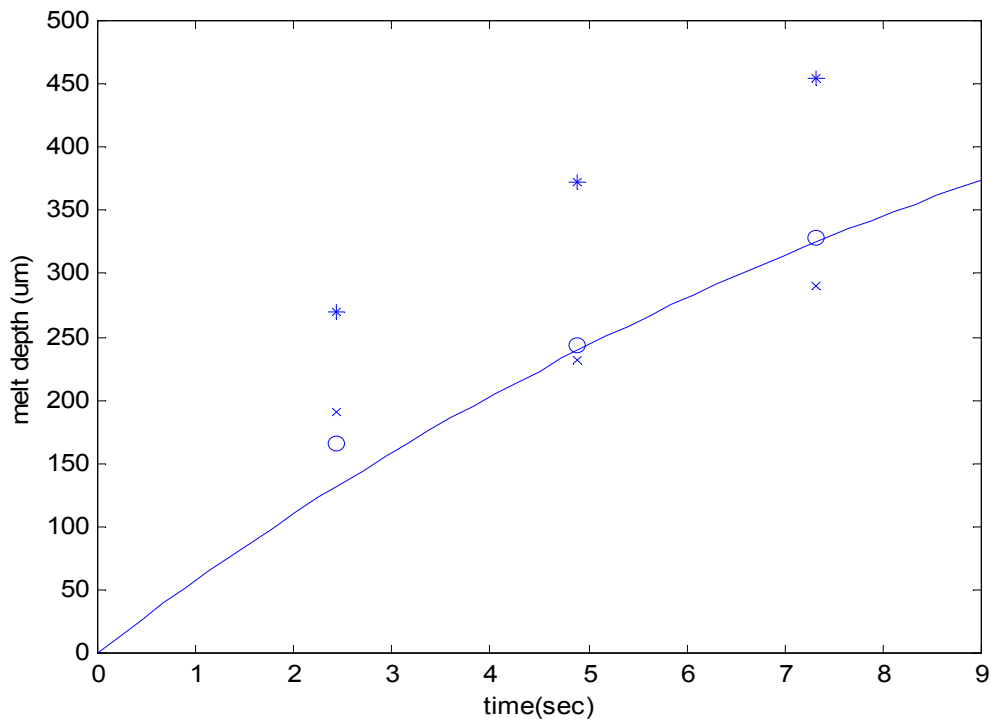


Fig.5: Melt depth as a function of interaction time (P=550W)

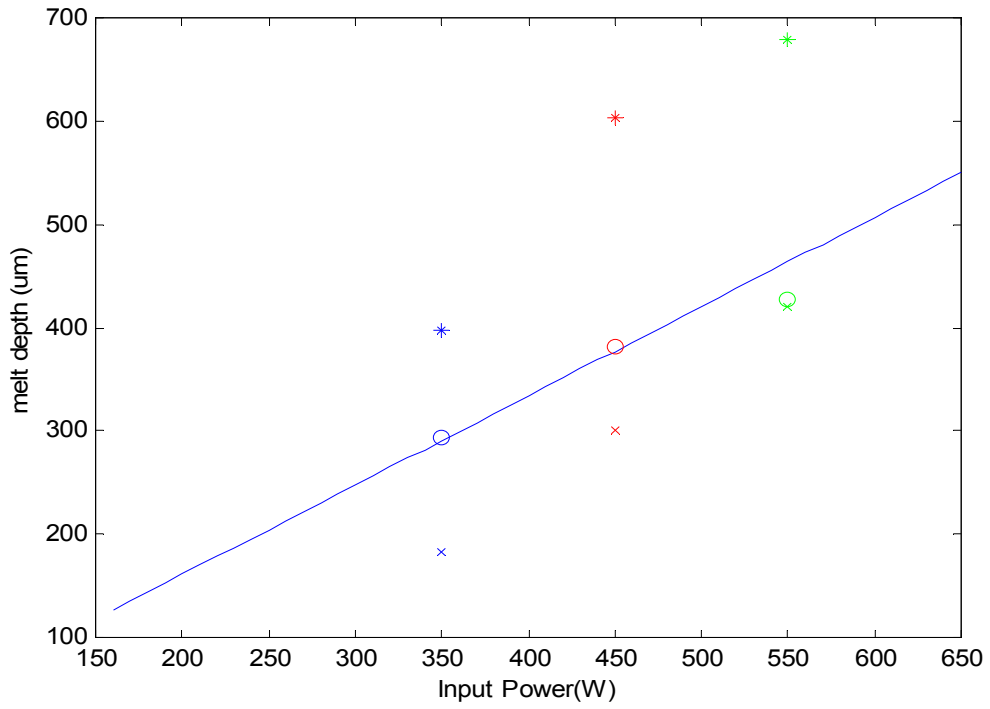


Fig.6: Melt depth as a function of power input ($V_s=0.27$ mm/s)

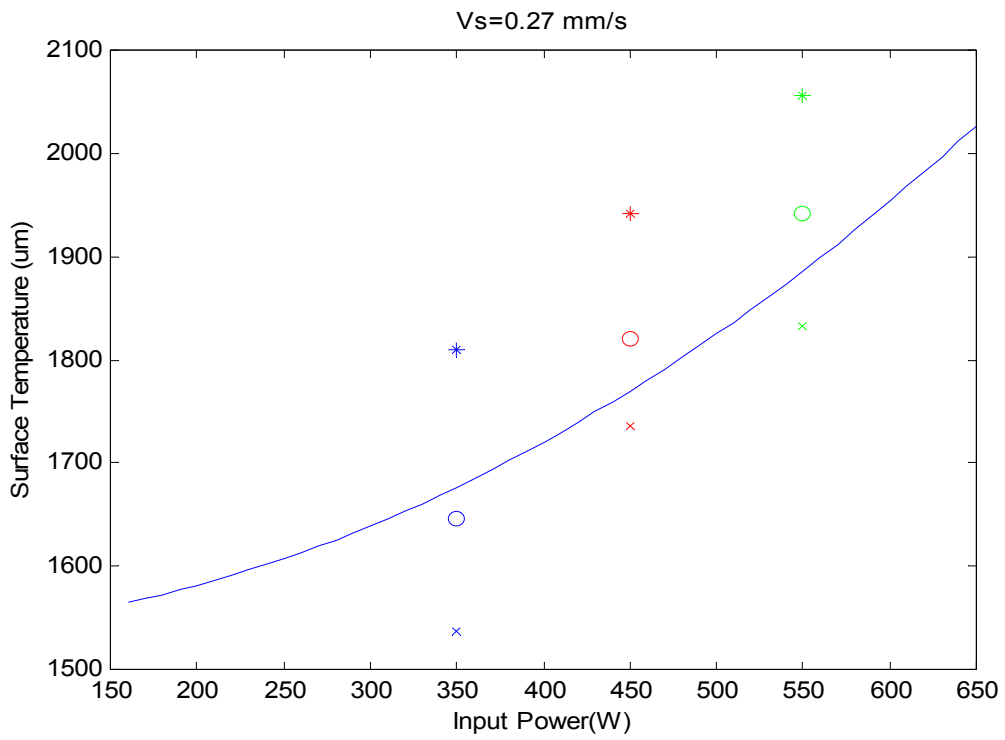


Fig.7: Surface Temperature as a function of Power Input

Figure 6 shown below depicts the relationship between melt depth and input power at three different power levels. As mentioned previously, three cross-sections were taken and the melt depth measured. The symbols shown represent the following: “x”- beginning of scan; “o” - middle of scan; “*” - end of scan. The plot shows the melt depth increases when the power is increased. The melt depth also increases within a single scan as the heat builds up, similar to the previous experiments. The solid line represents the results of the simulation, and again the model fits the data well for the measurements taken at the middle cross section. At the beginning of the scan, the model overestimates the melt depth, and at the end of the scan, the model underestimates the depth.

Figure 7 illustrates the relationship between input power and surface temperature for a constant scan speed. The surface temperature is clearly increasing as the power is increased. The trend appears to be exponentially increasing with power. The surface temperature values from the model and the data appear to follow the same exponential trends, but the model is sensitive to changes in absorptivity. This makes it difficult to calibrate due to the lack of absorptivity data in the liquid regime and the model cannot currently include absorptivity as a function of temperature.

Conclusions

1. Remote temperature measurement using short wave pass filter (dichroic filter) and pyrometer was proven feasible and effective as a means of providing real-time feedback information necessary for closed loop control.
2. Integrating two model approaches resulted in connecting surface melt temperature to melt depth.
3. The results of melt depth and temperature measurement experiments followed trends predicted by the model.
4. Heat buildup due to finite specimen dimensions and slow scan speeds results in increasing model error as the scan progresses.
5. Heat buildup will be significantly less in real applications due to much faster processing times.
6. Thermal model sacrifices its capability to handle boundary condition such as insulated wall for the sake of ease of implementation. However, the model results provided enough information to control the overall process by closed-loop feedback control scheme.
7. Transfer functions for SISO PID controller design were found and will be used to implement the feedback control system.

References

1. W. M. Steen, “Laser Material Processing”, 2nd Ed., Springer-Verlag, London, 1998.
2. S. Ahn, J. Murphy, J. A. Ramos, J. J. Beaman, “Physical modeling for dynamic control of melting process in direct-SLS,” Proceedings of the 12th Annual Solid Freeform Fabrication Symposium, Austin, TX, 591-598, August, 2001.
3. D. I. Pantelis, K. N. Vonatsos, “Development and experimental validation of analytical thermal models for the evaluation of the depth of laser-treated zones,” Appl. Phys. A, 67, 435-439, 1998.

4. J. Xie and A. Kar, "Mathematical modeling of melting during laser materials processing," J. Appl. Phys., 81(7), 3015-3022, 1997.
5. A. Ghosh, A. K. Mallik, "Manufacturing Science," 1st Ed., EWP, New York, 1986.

Acknowledgements

The Laboratory for Freeform Fabrication gratefully acknowledges the support of the Office of Naval Research for funding the project "Surface Engineering for SFF Processes," Grant No: N00014-00-1-0334.